Thermal Dissociation of the Protein Homodimer Ecotin in the Gas Phase

Natalia Felitsyn,* Elena N. Kitova, and John S. Klassen
Department of Chemistry, University of Alberta, Edmonton, Alberta, Canada

The influence of charge on the thermal dissociation of gaseous, protonated, homodimeric, protein ecotin ions produced by nanoflow electrospray ionization (nanoES) was investigated using the blackbody infrared radiative dissociation technique. Dissociation of the protonated dimer, $(E_2 + nH)^{n+} \equiv E_2^{n+}$ where $n = 14–17$, into pairs of monomer ions is the dominant reaction at temperatures from 126 to 175 °C. The monomer pair corresponding to the most symmetric charge distribution is preferred, although 50–60% of the monomer product ions correspond to an asymmetric partitioning of charge. The relative abundance of the different monomer ion pairs produced from E_2^{14+}, E_2^{15+}, and E_2^{16+} depends on reaction time, with the more symmetric charge distribution pair dominating at longer times. The relative yield of monomer ions observed late in the reaction is independent of temperature indicating that proton transfer between the monomers does not occur during dissociation and that the different monomer ion pairs are formed from dimer ions which differ in the distribution of charge between the monomers. For E_2^{17+}, the yield of monomer ions is independent of reaction time but does exhibit slight temperature dependence, with higher temperatures favoring the monomers corresponding to most symmetric charge distribution. The charge distribution in the E_2^{15+} and E_2^{16+} dimer ions influences the dissociation kinetics, with the more asymmetric distribution resulting in greater reactivity. In contrast, the charge distribution has no measurable effect on the dissociation kinetics and energetics of the E_2^{17+} dimer. (J Am Soc Mass Spectrom 2002, 13, 1432-1442) © 2002 American Society for Mass Spectrometry

Protein complexes composed of two or more subunits are believed to constitute the bulk of soluble and membrane-bound proteins [1, 2]. While the importance of protein assemblies in cellular function is well recognized, their structural characterization remains a significant analytical challenge. Mass spectrometry (MS), with its speed, sensitivity, and accurate mass capability holds tremendous potential as a tool for characterizing protein assemblies [3]. The use of multiple stages of MS with ion activation/dissociation (MS^n) to dissect gaseous assemblies into their constituent subunits represents an attractive, yet unproven, strategy for determining subunit composition and topology. In recent years, a number of MS^n studies of gaseous protein dimers [4, 5], tetramers [6], and pentamers [7] have been reported. Homo- and heterodimers are readily decomposed into their individual subunits, most generally by collision-induced dissociation (CID). An interesting feature of the dissociation behavior of the protein–protein complexes is the tendency for uneven sharing of charge between subunits, even in the case of homodimers. For example, the decomposition of four homodimers (human galectin I, *E. coli* glyoxalase I, horse heart cytochrome *c*, and hen egg lysozyme) yields a highly asymmetric charge distribution, with one of the subunits retaining as much as 73% of the dimer ion charge [4]. Even more pronounced charge state asymmetry is observed in CID experiments performed on cytochrome *c*-cytochrome b_5 complexes [5]. Cytochrome *c* retains as much as 90% of the total charge. Higher order oligomeric protein complexes, containing more than two subunits, dissociate by the loss of a single subunit that retains a disproportionately large fraction of the total charge [6–8]. The resulting oligomeric product ions are resistant to further dissociation, presumably due to the reduced charge-to-subunit ratio relative to the original complex.

The stability of the oligomeric product ions limits the amount of structural information that can be extracted from the MS^n experiments. Furthermore, the tendency for the oligomeric complexes in the gas phase to lose a single subunit may not reflect the nature of binding in solution. For example, in the gas phase the tetrameric assemblies of adult human hemoglobin and concanavalin dissociate via the loss of a single subunit [6], while in solution they are formed by the association of two specific dimers, rather than by the association of individual subunits. Similar asymmetric dissociation behavior is reported in a recent study [7] of the thermal decomposition of a gaseous multiply protonated ho-

Published online November 7, 2002

Address reprint requests to Dr. J. S. Klassen, Department of Chemistry, University of Alberta, Edmonton, Alberta T6G 2G2, Canada. E-mail: john.klassen@ualberta.ca

*Current address: College of Medicine, University of Florida, Gainesville, FL 32610-0277.

1044-0305/02/$20.00
PII S1044-0305(02)00647-5

Received May 2, 2002
Revised August 14, 2002
Accepted August 14, 2002

mopentamer (B_5) complex using the blackbody infrared radiative dissociation (BIRD) technique [9]. Dissociation of the pentamer proceeds by the loss of a single subunit, which retained 30–50% of the total charge.

The origin of the asymmetric charge distribution observed in the dissociation products of protein assemblies is not yet fully understood. An asymmetric charge distribution between subunits may be a consequence of the electrospray (ES)/desolvation process. Alternatively, proton transfer between protein subunits may occur upon excitation of the complexes. If proton transfer does occur, then the mobility of the protons is expected to be sensitive to the internal energy of the ions. In the recent BIRD study of the B_5 pentamer, it was shown that the degree of charge enrichment of the subunit that was lost was sensitive to the reaction temperature, with higher temperature favoring enrichment [7]. Based on this result it was concluded that at least some of the protons were able to migrate in the gas phase between the subunits and account for the observed enrichment of charge on the leaving subunit. However, the occurrence of charge migration does not exclude the possibility that the ES/desolvation process also contributes to the formation of an asymmetric charge distribution.

Clearly, a better understanding of the effects of desolvation on protein gas phase structure and of the relationship between charge and dissociation mechanism is necessary if gas phase dissociation experiments are to be successfully used to deduce the information about composition and solution structure of protein assemblies. In an effort to gain a better understanding of the origin of the asymmetric dissociation behavior of gaseous proteins assemblies, our laboratory has undertaken an investigation of the dissociation pathways, kinetics and energetics of a number of protein complexes using BIRD. Here, we report results obtained for the protein homodimer ecotin, a serine proteases inhibitor expressed by *E. coli* [10]. Each monomer is comprised of 142 amino acids arranged as an antiparallel seven-stranded β-barrel (Figure 1) [11]. The ecotin dimer has a dissociation constant of approximately 400 nM [12] and has been shown to retain its inhibitory activity after exposure to high temperatures (100 °C) and highly acidic conditions (pH 1) [9, 13]. In solution, the monomers interact predominantly through the C-terminal ends (residues 125–142), which form a two-stranded antiparallel β-sheet [13]. There are 10 hydrogen bonds between the subunits, eight of which are in the C-terminal region. Two salt bridges between NH1 of C-terminal Arg 142 and OE1 of N-terminal Glu 2 further stabilize the dimer in solution. In the gas phase, hydrogen bonds are expected to be the dominant interactions stabilizing the dimer [7, 14]. The time-resolved BIRD experiments were used to determine the temperature dependence of the rate constants for the dissociation of the dimer into monomers and thereby the Arrhenius activation parameters. The BIRD data were also used to evaluate the influence of temperature and reaction extent on the charge states of the monomer product ions and to identify the charge distribution within the dimer ions.

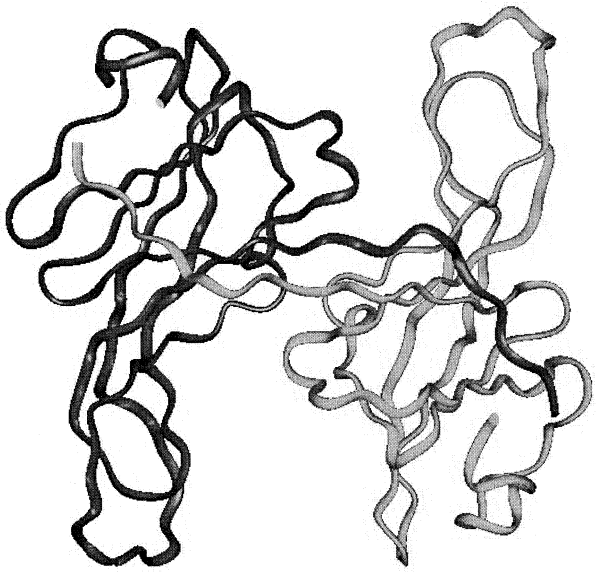

Figure 1. Crystal structure of the ecotin dimer.

Experimental

The experimental apparatus and procedures used in this work have been described in detail elsewhere [7] and only a brief overview is given here. All experiments were performed on an ApexII 47e Fourier transform ion cyclotron resonance (FT-ICR) mass spectrometer (Bruker, Billerica, MA) equipped with a modified external nanoelectrospray ion source. The gaseous protein ions were produced by nanoflow electrospray ionization (nanoES). The nanoES tip was constructed from an aluminosilicate capillary (0.68 mm i.d., 1.0 mm o.d.) pulled at one end to ~5 μm o.d. and 1–3 μm i.d. with a micropipette puller. A voltage of 800–1000 V was applied to a platinum wire inserted inside the nanoES tip. Ecotin was purchased from Sigma Canada and used without further purification. The protein was dissolved in either 1 mM aqueous ammonium acetate (pH 6.8) or 5 mM acetic acid (pH 3.5) at a concentration of 2.0 μM. A heated stainless steel capillary was used to sample the gaseous ions and droplets produced by nanoES into the vacuum chamber of the mass spectrometer. Ions were accumulated in the external hexapole for 1–3 s, then ejected and accelerated to ~2700 V through the fringing field of the 4.7 T magnet, decelerated and introduced into the heated ion cell. The temperature of the ion cell was controlled by two external flexible heating blankets placed around the vacuum tube in the vicinity of the ion cell. Mass spectra were acquired by an SGI R5000 computer running the Bruker Daltonics XMASS software, version 5.0. On average 20 scans, containing 128 K data points per scan, were acquired per spectrum.

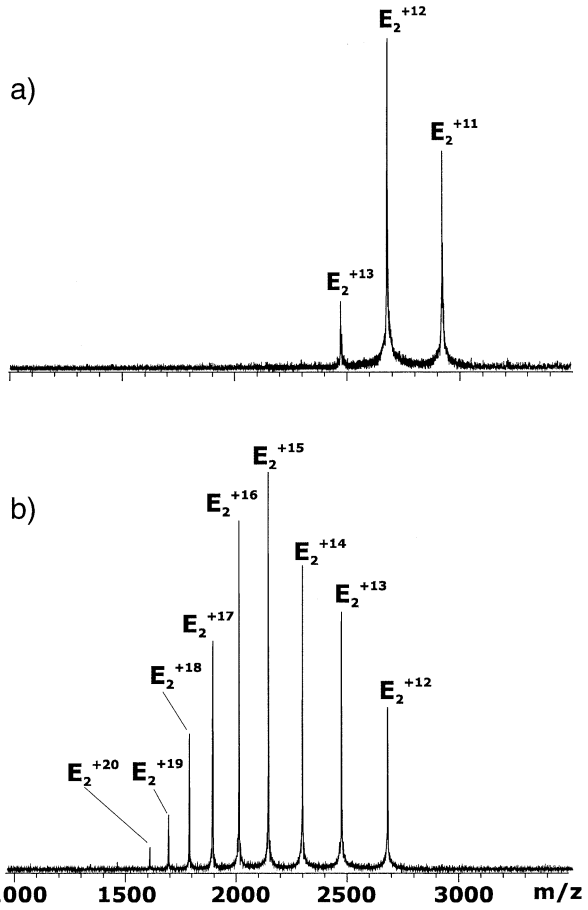

Figure 2. Nanoelectrospray mass spectra of a 2.0 μM aqueous solution of ecotin and (**a**) 1 mM ammonium acetate (pH = 6.8), and (**b**) 5 mM acetic acid (pH = 3.5).

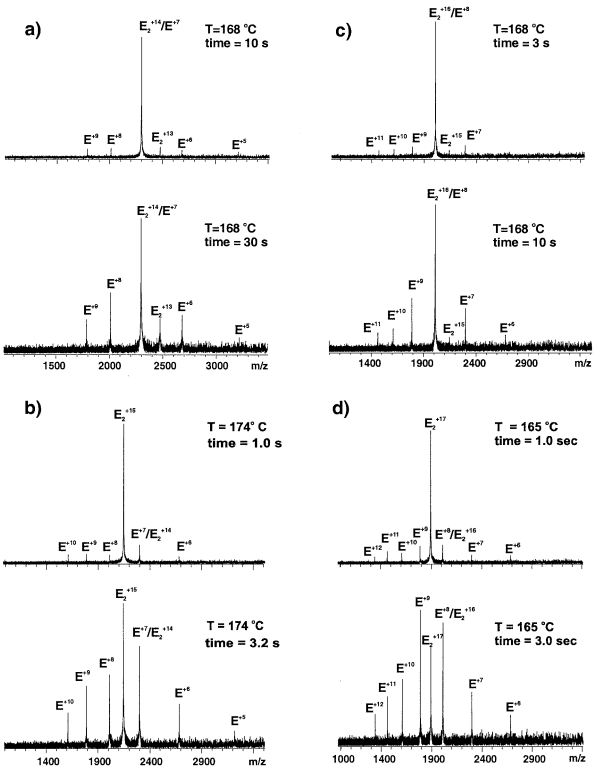

Figure 3. Blackbody infrared radiative dissociation spectra of E_2^{n+} ions: (**a**) E_2^{14+}, 168 °C, 10 s and 30 s; (**b**) E_2^{15+}, 174 °C, 1.0 s and 3.2 s; (**c**) E_2^{16+}, 168 °C, 3 s and 10 s; and (**d**) E_2^{17+}, 165 °C, 1.0 s and 3.0 s.

Results and Discussion

NanoES of Ecotin

NanoES of aqueous solutions containing 2 μM ecotin and 1mM ammonium acetate (pH 6.8) produced exclusively ecotin dimer ions, E_2^{n+} where n = 11–13 (Figure 2a). At these charge states, the dimer ions undergo very little dissociation at the highest temperature accessible with the experimental apparatus (175 °C) and reaction times as long as 300 s. In a previous BIRD study of a B_5 protein complex, it was shown that the kinetic stability of the complex decreased with increasing charge state [7] and a similar trend in reactivity was found for the ecotin dimer ions in the present work. To produce dimers with higher charge states, the nanoES solution was acidified to pH 3.5 by the addition of acetic acid. Acidification resulted in a broadened distribution of dimer charge states, which ranged from +12 to +20 (Figure 2b). The higher charge states and broadened charge envelope are both indicative of acid-induced denaturation of the monomers. However, little or no monomer ions were observed under these conditions indicating that the loss of higher order structure did not result in a significant loss in stability of the dimer in solution. Also, the +12 and +13 ions produced from the acidified solution were not found to be any more reactive than the +12 and +13 ions produced from neutral solution. Under both the neutral and acidic conditions, protons were found to be the dominant charging agent, although a small fraction (<20%) of the E_2^{n+} ions contained one or more Na^+ ions.

Reaction Pathways

BIRD was performed on the protonated dimer ions, E_2^{n+} where n = 14–17, at temperatures ranging from 126 to 175 °C. At these temperatures, the dominant reaction involved dissociation of the dimer into monomers (eq 1):

$$E_2^{n+} \rightarrow E^{(n-a)+} + E^{a+} \quad (1)$$

Representative BIRD spectra, acquired for each E_2^{n+} ion at a given temperature and two different reaction times, are shown in Figure 3. Dissociation of the E_2^{n+} ions produced as many as four pairs of monomers with complementary charge states (i.e., $E^{(n-a)+}/E^{a+}$). Dissociation of the E_2^{15+} and E_2^{17+} ions produced a monomer ion pair with a nearly symmetric distribution of charge (E^{8+}/E^{7+} and E^{9+}/E^{8+}) and pairs with a more asymmetric distribution of charge (E^{10+}/E^{7+}, E^{11+}/E^{6+}, E^{12+}/E^{5+} and E^{9+}/E^{6+}, E^{10+}/E^{5+}), see Scheme **1**. The

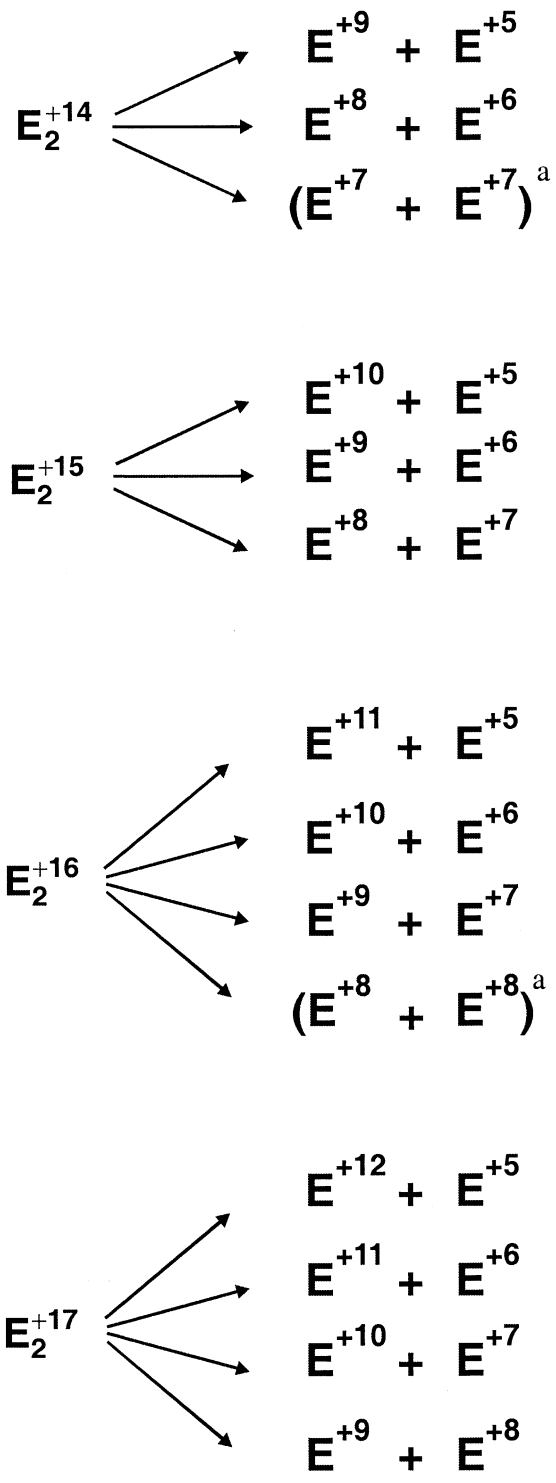

Scheme 1. Monomer charge states observed from the dissociation of the E_2^{n+} ions (n = 14–17). These ions have an m/z coincidental with that of the dimer ion.

E^{5+} ion was sometimes absent from the BIRD spectrum, despite the presence of its complementary ion, due to low charge state and concomitant lower detection efficiency. For E_2^{14+} and E_2^{16+}, the monomers corresponding to equal sharing of the charge (i.e., E^{7+} and E^{8+}, respectively) have the same m/z as the dimer ion and therefore, their relative abundance could not be determined directly from the mass spectrum. However, it was possible to estimate the relative abundance of the symmetric charge products from the BIRD spectra obtained at long reaction times where it is assumed that the dimer was completely dissociated and that any ions remaining at the same m/z corresponded to the monomer ions. Using this approach, the symmetric products were estimated to account for ~40% of the product ions. From the BIRD spectra shown in Figure 3 it can also be seen that the relative yield of the different monomer pairs was sensitive to the reaction time. Early in the reaction, the intensities of the different monomer pairs were similar, whereas at longer times the monomer pair corresponding to the more symmetric charge distribution dominated. For a given dimer charge state, it was also found that the relative yield of each monomer pair decreased with increasing charge asymmetry. For example, the E^{12+}/E^{5+} pair, which is the most asymmetric pair produced from E_2^{17+} and corresponds to the retention of 71% of the dimer charge by one of the monomers, represented only ~15% of the product ions. In contrast, the most charge-symmetric monomer pair, E^{9+}/E^{8+}, represented ~42% of the product ion intensity (see Table 1).

Table 1. Normalized abundance of the monomer ions produced from the dissociation of ecotin dimer ions E_2^{n+} obtained near complete reaction and averaged over all temperatures

Dimer	Products	A_i^{max}
E_2^{+14}	$E^{+7} + E^{+7}$	0.36 ± 0.07
	$E^{+8} + E^{+6}$	0.45 ± 0.08
	$E^{+9} + E^{+5}$	0.19 ± 0.02
E_2^{+15}	$E^{+8} + E^{+7}$	0.51 ± 0.03
	$E^{+9} + E^{+6}$	0.37 ± 0.03
	$E^{+10} + E^{+5}$	0.12 ± 0.02
E_2^{+16}	$E^{+8} + E^{+8}$	0.37 ± 0.05
	$E^{+9} + E^{+7}$	0.41 ± 0.04
	$E^{+10} + E^{+6}$	0.14 ± 0.02
E_2^{+17}	$E^{+11} + E^{+5}$	0.08 ± 0.02
	$E^{+9} + E^{+8}$	0.42 ± 0.09
	$E^{+10} + E^{+7}$	0.22 ± 0.03
	$E^{+11} + E^{+6}$	0.18 ± 0.06
	$E^{+12} + E^{+5}$	0.17 ± 0.08

In addition to the dissociation reaction leading to monomers (eq 1), the dimer ions also undergo the loss of one or more small neutrals (N) with a mass of approximately 18 Da, i.e., H_2O or NH_3 (see Figure 4). The loss of both H_2O and NH_3 has been previously observed in the BIRD and CID spectra of protonated peptides and proteins [15]. The sequential loss of neutrals resulted in a distribution of dimer and monomer ions at a given charge state (e.g., E_2^{n+}, $[E_2 - N]^{n+}$, $[E_2 - 2N]^{n+}$ and E^{a+}, $[E - N]^{a+}$, $[E - 2N]^{a+}$), Scheme **2**.

The E_2^{n+} ions also undergo charge loss, resulting in the appearance of $E_2^{(n-1)+}$ ions in the spectrum. The charge-loss reaction may be the result of a bimolecular process whereby charge is transferred from the dimer to

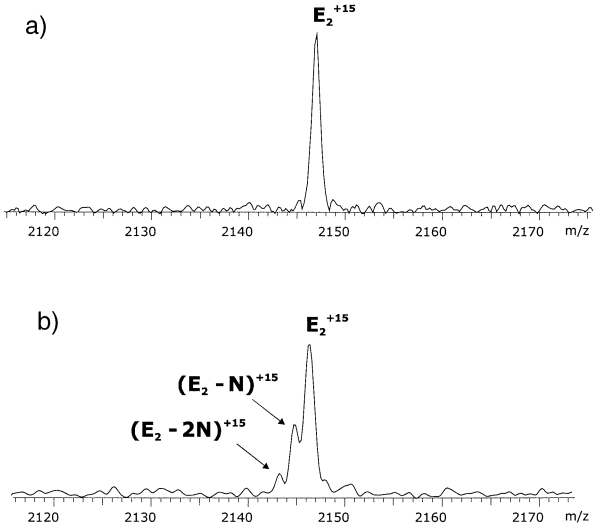

Figure 4. Blackbody infrared radiative dissociation spectra of E_2^{15+} ions: (**a**) 144 °C, 0 s and (**b**) 144 °C, 90 s.

neutrals present in the vacuum chamber. Alternatively, charge loss may be unimolecular in nature, proceeding by the loss of charged, low molecular weight species. Based on the similarity in the masses determined for the E_2^{14+} and E_2^{16+} ions and their respective charge loss products, it was concluded that a bimolecular mechanism is responsible for the majority, if not all, of the charge loss reaction. In the case of the even charge state dimers, the $E_2^{(n-1)+}$ ion could be directly observed in the mass spectrum. The normalized abundance (charge normalized intensity) of the charge-loss product of E_2^{16+} was found to be approximately 4–5% of the total product ion abundance. Charge loss was more significant for the E_2^{14+} ion; at long reaction times, the normalized intensity of E_2^{13+} accounted for ~20% of the product ion abundance. The larger contribution of this reaction is attributed to the greater kinetic stability of the E_2^{14+} dimer, compared with the higher charge state dimers investigated. The $E_2^{(n-1)+}$ ions were also able to undergo secondary dissociation reactions. However, as discussed in a preceeding section, the dissociation rate constants for the $E_2^{(n-1)+}$ ions are approximately 2 to 4 times smaller than for E_2^{n+}. As a result of the smaller dissociation rate constant and low abundance, dissociation of the $E_2^{(n-1)+}$ ion contributed little to the abundance of the monomer ions. For the odd charge state E_2^{n+} ions (n = 15 and 17), the m/z of the $E_2^{(n-1)+}$ ion coincides with that of one of the monomer product ions and, consequently, the relative abundance of the monomer and $E_2^{(n-1)+}$ ions could not be directly measured. However, it could be estimated from the abundance of the complementary monomer ion. Using this approach, the charge-normalized abundance of the monomer ion accounted for ~95% of the observed abundance, with the remaining 5% due to the charge loss product, $E_2^{(n-1)+}$.

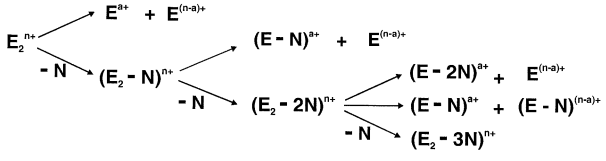

Scheme 2. Possible reaction scheme for the dissociation of E_2^{n+} ions into monomer ions or by loss of a neutral (N).

Dependence of Monomer Ion Abundance on Reaction Time and Temperature

As illustrated in Figure 3, the relative intensity of the monomer ion pairs produced by the dissociation of E_2^{n+} ions varied with reaction time. This dependence is more clearly seen by plotting the normalized abundance of the monomers, $A_{i,rel}$, relative to the sum of all the product ions, versus reaction time (Figure 5). $A_{i,rel}$ was calculated using the following expression:

$$A_{i,rel} = A_i / \sum A_{M'} \quad (2)$$

where A_i is the measured abundance of a given monomer ion and $\Sigma A_{M'}$ is the sum of the abundance of all the monomer ions. Due to the difficulty in detecting the E^{5+} and, in some cases, the E^{6+} ions and the coincidental m/z's of one of the monomers and the $E_2^{(n-1)+}$ ion, only the abundance of one monomer, with charge greater than half of the parent ion charge, per product ion pair was considered. For the E_2^{14+} and E_2^{16+} ions, these plots only include the monomer pairs that correspond to an asymmetric charge distribution because the abundance of the E^{7+} and E^{8+} ions, respectively, could not be determined during the reaction.

For the E_2^{14+}, E_2^{15+}, and E_2^{16+} ions, $A_{i,rel}$ of the monomer corresponding to the most symmetric charge distribution (that could be observed) increased as the reaction proceeded, at the expense of the monomers with the more asymmetric charge distributions (Figure 5a, b, and c). However, for E_2^{17+} the $A_{i,rel}$ of the monomer ions was found to be essentially constant over the entire reaction (Figure 5d).

Proton transfer within the dimer, from the higher to lower charge state monomer, during dissociation could account for the change in $A_{i,rel}$ with reaction time observed for the E_2^{14+}, E_2^{15+}, and E_2^{16+} ions. Proton transfer between protein subunits was shown to occur during dissociation of a B_5^{n+} pentamer complex [7]. For that complex, the degree of charge enrichment was sensitive to the reaction temperature, with higher temperatures promoting enrichment. Alternatively, the change in $A_{i,rel}$ with reaction time could be due to the presence of E_2^{n+} ions with different charge distributions and correspondingly distinct dissociation rate constants. Douglas and coworkers have previously proposed the existence of multiple protein dimer conformations with different reactivity [5]. To establish whether proton migration was responsible for the preferential formation of monomer ions with a more sym-

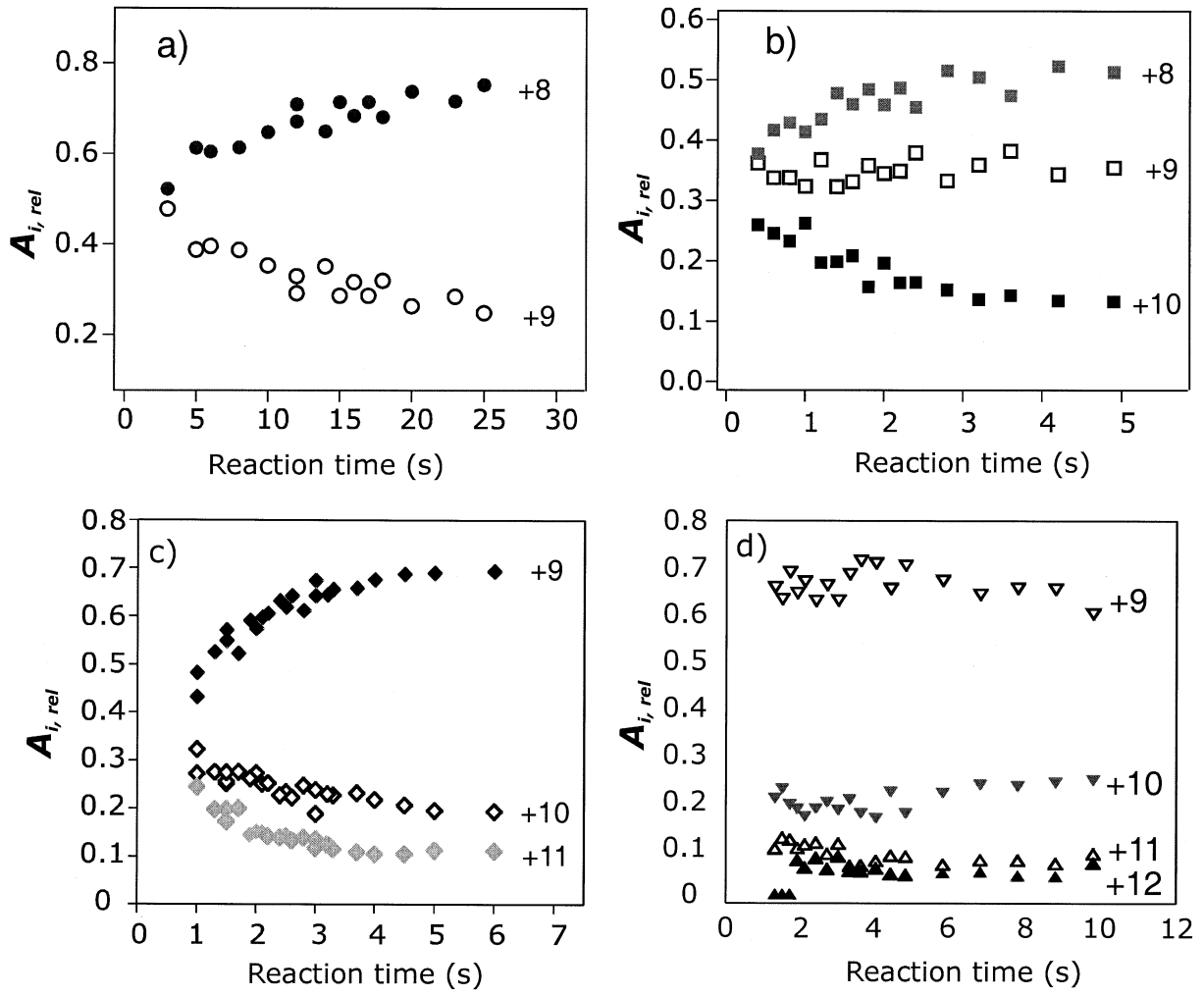

Figure 5. Plots of normalized abundance of the monomer product ions, $A_{i,rel}$, *versus time for the dimer ions: (***a***)* E_2^{14+}, 173 °C; (**b**) E_2^{15+}, 174 °C; (**c**) E_2^{16+}, 173 °C, and (**d**) E_2^{17+}, 160 °C.

metric charge distribution, the $A_{i,rel}$ values corresponding to the monomer pairs from E_2^{15+}, E_2^{16+} and E_2^{17+} measured late in the reaction (i.e., A_i^{max}) were plotted versus reaction temperature (Figure 6). Although there is scatter in the data, the A_i^{max} values for the different monomer ions of E_2^{15+} and E_2^{16+} were largely insensitive to the reaction temperature (Figure 6a). The plots of A_i^{max} for the different monomer ions produced from E_2^{17+} were much more scattered (Figure 6b). Despite the scatter, the data suggested that A_i^{max} was slightly dependent on temperature, with higher reaction temperatures favoring the monomer pair with the most symmetric charge distribution (i.e., E^{9+}/E^{8+}).

The lack of temperature dependence in the A_i^{max} values obtained for the E_2^{15+} and E_2^{16+} ions suggests that proton transfer between monomers did not occur appreciably during the dissociation process. Therefore, it was concluded that these dimer ions consisted of three or four *charge isomers*, differing in the charge distribution between monomers (e.g., $E_2^{+n} \equiv E^{(n-a)+} \cdot E^{a+}$, $E^{(n-b)+} \cdot E^{b+}$, . . .) and relative abundance. The change in $A_{i,rel}$ with reaction time observed for the E_2^{15+}, E_2^{16+} and, presumably, E_2^{14+} ions can be explained by the differential reactivity and abundance of each charge isomer, see Scheme **3**. As described in more detail in a preceeding section, the reactivity of the E_2^{15+} and E_2^{16+} ions was sensitive to the charge distribution, with charge isomers with an even or near-even charge distribution being less reactive (but more abundant) than isomers with a more asymmetric distribution of charge. Consequently, early in the reaction the abundance of the more charge-asymmetric monomers was greater due to the lower stability of the corresponding dimer. As the reaction proceeded, the dimers with a more asymmetric charge distribution were depleted and the relative abundance of monomer product ions reflects the relative abundance of the charge isomers from which they were formed. In other words, at long reaction times, the relative abundance of the monomer ions reflects the original charge distribution in the dimer ions.

The E_2^{17+} ion is also believed to be a collection of charge isomers. In contrast to the behavior of the lower charge state dimers, there is evidence that proton transfer between monomers can alter the charge distribution,

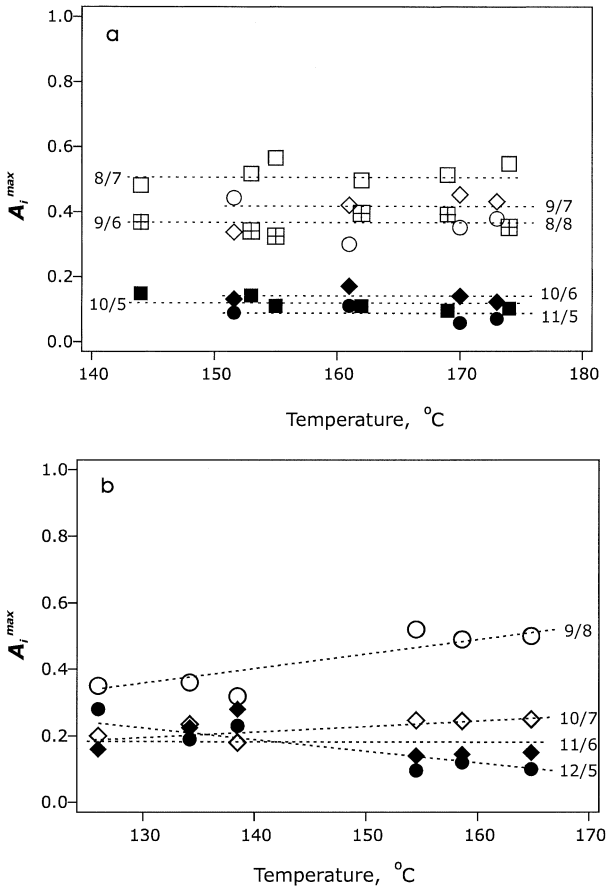

Figure 6. Plots of normalized abundance of the monomer product ions, determined near complete reaction, versus temperature for the +15 to +17 charge states of E_2: (**a**) open square, E^{8+}/E^{7+} products of E_2^{15+}; hatched square, E^{9+}/E^{6+} products of E_2^{15+}; filled square, E^{10+}/E^{5+} products of E_2^{+15}; open diamond, E^{8+}/E^{8+} products of E_2^{16+}; open circle, E^{9+}/E^{7+} products of E_2^{16+}; filled diamond, E^{10+}/E^{6+} products of E_2^{16+}; filled circle, E^{8+} product of E_2^{16+}. (**b**) open circle, E^{9+}/E^{8+} product of E_2^{17+}; open diamond, E^{10+}/E^{7+} product of E_2^{17+}; filled diamond, E^{11+}/E^{6+} product of E_2^{17+}; filled circle, E^{12+}/E^{5+} product of E_2^{17+}.

with higher temperatures favoring a more symmetric distribution. The reason why proton transfer was possible for E_2^{+17} ion and not the other dimer ions is not clear but may reflect greater unfolding of the monomers due to the higher total charge, which could facilitate proton transfer.

In the absence of proton transfer between monomers

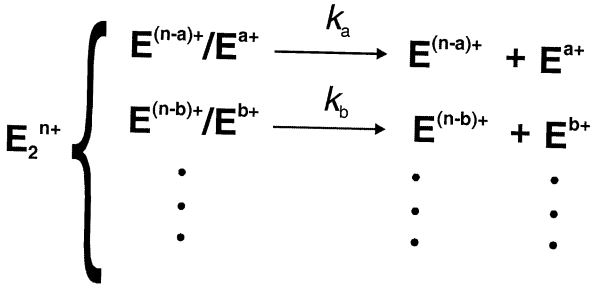

Scheme 3. Dissociation of the charge isomers of E_2^{n+} into monomer ions.

during the dissociation process, at least for the lower charge state ions, the BIRD spectra provide insight into the charge distribution established by the nanoES ion source. Listed in Table 1 are the A_i^{max} values for the different monomer ion pairs produced from E_2^{14+}, E_2^{15+}, E_2^{16+}, and E_2^{17+}, averaged over all of the temperatures investigated. The even or near-even charge isomer, which is expected to dominate for structurally identical proteins, accounts for 40–50% of the dimer ions. Dimers with the next most symmetric distribution were also present in high abundance. In fact, the two isomers with the most symmetric charge distributions account for ~80% of all the dimer ions. The origin of the remaining 20% of the dimer ions in which the charge is distributed in a highly asymmetric fashion is intriguing. The nanoES/desolvation process may be solely responsible for dimer ions with an asymmetric distribution of charge, although thermally-assisted proton transfer within the ion source may also influence the final distribution of charge. The mechanism(s) by which proteins and other biopolymers are charged during the electrospray (ES) process is not fully understood. In the case of globular proteins, it is generally accepted that the charge residue model [16, 17], wherein charges on the surface of the ES droplets containing a single protein molecule are transferred to the protein during the final stages of desolvation, operates. Assuming this is the dominant mechanism for the production of charged gaseous ecotin ions, one can speculate as to the origin of the asymmetric charging. First, it is likely that portions of the complex become desolvated before others. Since the charge is expected to remain with the solvation layer, this "uneven" desolvation could lead to concentration of charge on one of the monomers. Alternatively, the uneven charging may result from structural differences between the monomers in solution. In a recent review of X-ray structures of homo-oligomeric enzymes, it was noted that conformational differences between subunits were common features [18]. Proton transfer, driven by collisional heating in the ion source, may also influence the structure and charge distribution of the ions. However, this explanation does not seem likely in the case of ecotin, at least for the +17 ions, since higher cell temperatures were found to favor a more symmetric distribution of charge.

Thermal Dissociation Kinetics

One of the objectives of this work was to evaluate the influence of charge on the kinetics and energetics for the dissociation of the dimer into monomers (eq 1). Extracting the temperature dependent rate constants from the BIRD data was complicated by several factors. These difficulties are described below, along with the approach used to estimate the dissociation rate constants for the E_2^{14+}, E_2^{15+}, E_2^{16+}, and E_2^{17+} ions.

Shown in Figure 7 are the kinetic data measured for the dissociation of the E_2^{15+} and the E_2^{17+} ions at several temperatures. The natural log of the normalized abun-

dance of the dimer, $A_{D,norm}$, is plotted versus reaction time, along with a linear least squares fit of part or all of the kinetic data. The normalized abundance of the E_2^{15+} and E_2^{17+} ions was calculated using the expression:

$$A_{D,norm} = A_D/(A_D + \sum A_{M'}) \quad (3)$$

where A_D is the measured abundance of the dimer ion and $A_{M'}$ is the abundance of one monomer of each ion pair. Since the dissociation reaction occurred in parallel with the charge- and neutral-loss reactions, the contribution of these additional reactions to the rate of dimer ion loss had to be considered. It was possible to account for the neutral loss reactions by assuming that it did not influence the reactivity of the dimer. The abundance of the dimer and monomer ions at a given charge state, having lost one or more neutrals, was simply added to the abundance of dimer and monomer ions which had not undergone neutral loss. The summed abundance was then used in the calculation of $A_{D,norm}$. The charge loss reaction leading to the $E_2^{(n-1)+}$ ion could not be included in the rate constant calculation because the $E_2^{(n-1)+}$ ion coincided with the *m/z* of one of the monomer ions. Fortunately, this reaction was only significant for the E_2^{14+} ion and omission of this process from the analysis of the kinetic data for the E_2^{15+} and E_2^{17+} ions has only a small effect on the magnitude of the rate constants.

For unimolecular reactions of a single reactant via multiple pathways, the plot of ln $A_{D,norm}$ versus time should be linear and the overall or average dissociation rate constant (k_{ave}) can be determined from the slope of the curve:

$$\ln(A_{D,norm}) = -k_{ave}\, t \quad (4)$$

At the reaction temperatures investigated, the kinetic plots obtained for E_2^{15+} appear to contain at least two components (Figure 7a). This behavior is consistent with the presence of several E_2^{15+} ions with distinct charge distributions (i.e., charge isomers) and distinct dissociation rate constant. The contribution of the more reactive isomers to the overall reaction rate will decrease with time (due to depletion of the reactant) and result in an apparent decrease in the reaction rate and nonlinear or multi-component kinetic plots. Due to the presence of multiple reactant ions, with different rate constants, it was not possible (or meaningful) to calculate k_{ave} for E_2^{15+}. Instead, the rate constant for the dissociation of each charge isomer was determined, vide infra. In contrast, the plots obtained for E_2^{17+} were linear at all temperatures investigated (Figure 7b) and k_{ave} was determined from the slope of a linear least squares fit of the kinetic data. The linear kinetic plots indicate that the dissociation rate constants for the four charge isomers (E^{9+}·E^{8+}, E^{10+}·E^{7+}, E^{11+}·E^{6+}, and E^{12+}·E^{5+}) are similar, at all temperatures investigated.

Similar kinetic plots could not be constructed for the

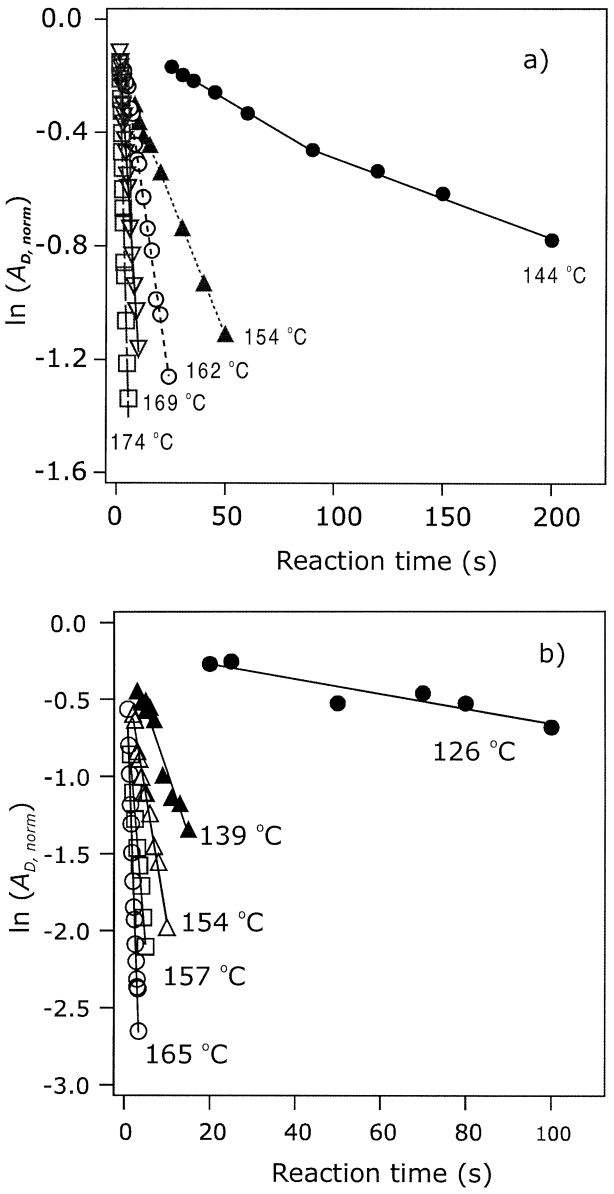

Figure 7. Kinetic data for the dissociation of (**a**) E_2^{15+} and (**b**) E_2^{17+}, fit to first-order kinetics at the temperatures indicated. In the case of E_2^{15+}, the kinetic data are composed of two linear segments.

E_2^{14+} and E_2^{16+} ions because the *m/z* of the monomer ion corresponding to a symmetric distribution of charge (i.e., E^{7+} and E^{8+}, respectively) coincides with that of dimer ion and $A_{D,norm}$ could not be determined from the BIRD spectra.

The dissociation rate constant (k_i) for individual reaction pathway, leading to a particular monomer ion pair, was calculated from the change in the normalized abundance of the high charge state monomer ion from each pair, $A_{M',norm}$, with reaction time using the following expression:

$$A_{M',norm} = A_{M',norm,max}(1 - exp(-k_i t)) \quad (5)$$

$A_{M',norm,max}$ is the normalized abundance of the mono-

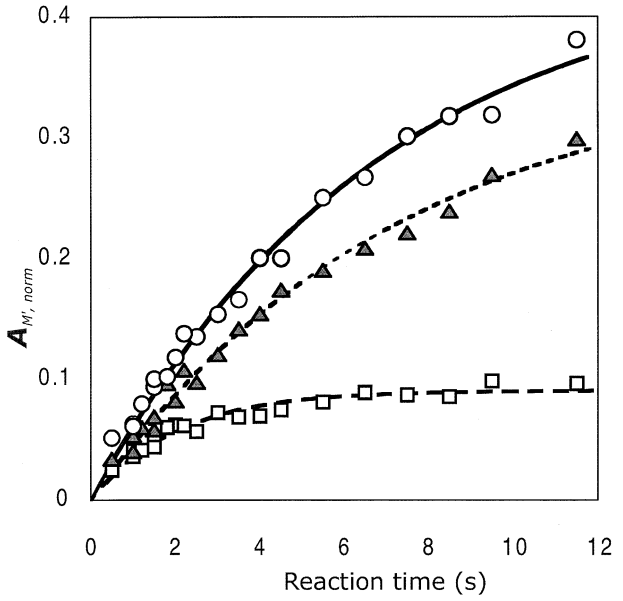

Figure 8. The normalized abundance of the monomer ions E^{8+} (open circle), E^{9+} (filled triangle), and E^{10+} (open square) produced from E_2^{15+} at 169 °C plotted versus time. Also shown is the nonlinear least squares fit of the data.

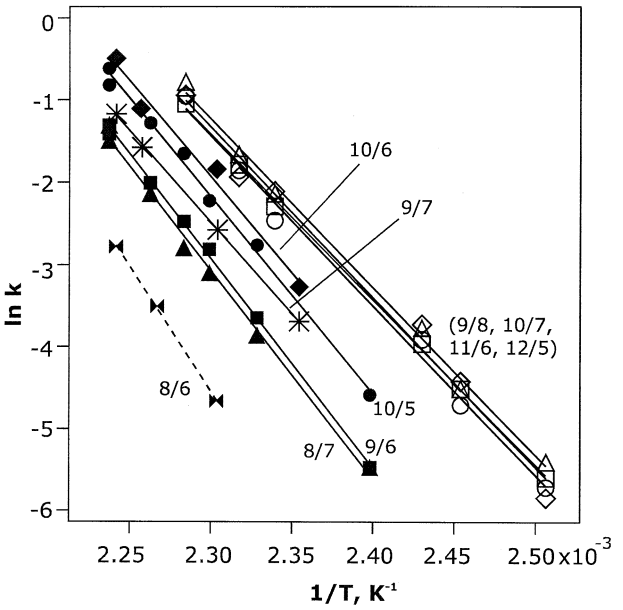

Figure 9. Arrhenius plots for the dissociation of the charge isomers $E^{8+}\cdot E^{6+}$ (filled butterfly), $E^{10+}\cdot E^{5+}$ (filled circle), $E^{9+}\cdot E^{6+}$ (filled triangle), $E^{8+}\cdot E^{7+}$ (filled square), $E^{9+}\cdot E^{7+}$ (large asterisk), $E^{10+}\cdot E^{6+}$ (filled diamond), $E^{12+}\cdot E^{5+}$ (open diamond), $E^{11+}\cdot E^{6+}$ (open triangle), $E^{10+}\cdot E^{7+}$ (open square), and $E^{9+}\cdot E^{8+}$ (open circle) ions.

mer determined at ~100% reaction.

For the E_2^{15+} and the E_2^{17+} ions, $A_{M',norm}$ was calculated by dividing the measured abundance of the monomer, $A_{M'}$, by the sum of abundance of the dimer and monomer ions:

$$A_{M',norm} = A_{M'}/(A_D + \sum A_{M'}) \quad (6)$$

For the E_2^{14+} and E_2^{16+} ions, $A_{M',norm}$ was calculated by an alternative method. The sum of the intensities of a given monomer pair ($I_M = I_{E^{(n-a)+}} + I_{E^{a+}}$) was divided by the sum of the intensities of the dimer and all the monomer product ions ($I_D + \Sigma I_M$):

$$A_{M,norm} = I_M/(I_D + \sum I_M) \quad (7)$$

This alternative method was necessary because the *m/z* of the charge-symmetric monomers is coincidental with the *m/z* of the dimer ion.

Illustrative plots of $A_{M',norm}$ versus reaction time for the three sets of monomer ions (E^{10+}/E^{5+}, E^{9+}/E^{6+}, and E^{8+}/E^{7+}) produced from E_2^{+15} at 169 °C are shown in Figure 8, along with a nonlinear least squares fit of the data. It can be seen that $A_{M',norm}$ for E^{10+} becomes constant much earlier in the reaction than it does for E^{9+} or E^{8+}, indicating that the dissociation rate constant for the $E^{10+}\cdot E^{5+}$ charge isomer is larger than for $E^{9+}\cdot E^{6+}$or $E^{8+}\cdot E^{7+}$, which exhibited similar rate constants. This behavior was observed at all temperatures investigated. A similar trend in dissociation rate constants was observed for the charge isomers of E_2^{16+}. For E_2^{17+}, however, the rate constants for the production of the different monomer pairs were found to be indistinguishable, within the experimental error, at all reaction temperatures investigated.

Rate constants were also determined at three temperatures (161, 168, and 173 °C) for the dissociation of the $E^{8+}E^{6+}$ isomer ion pair of the E_2^{14+} ion.

Arrhenius Dissociation Parameters

Arrhenius plots for the individual dissociation pathways of E_2^{14+}, E_2^{15+}, E_2^{16+}, and E_2^{17+} are shown in Figure 9. The Arrhenius activation energy (E_a) and preexponential factor (A) were determined from the slope and y-intercept, respectively, of the plots and the values are listed in Table 2. Reliable Arrhenius parameters could not be determined for E_2^{14+} because of the limited temperature range (12 °C) over which kinetic data were

Table 2. Arrhenius parameters for the dissociation of ecotin dimer into monomer ions ($E_2^{n+} \rightarrow E^{(n-a)+} + E^{a+}$)

Dimer	Products	E_a (kcal/mol)	A (s^{-1})
E_2^{+14}	$E^{+8} + E^{+6}$	(60)[a]	(10^{28})[a]
E_2^{+15}	$E^{+10} + E^{+5}$	47.5 ± 1.5	$10^{23.0\pm0.8}$
	$E^{+9} + E^{+6}$	50.6 ± 0.9	$10^{24.2\pm0.4}$
	$E^{+8} + E^{+7}$	50.4 ± 1.7	$10^{24.0\pm0.8}$
E_2^{+16}	$E^{+10} + E^{+6}$	46 ± 4	$10^{22\pm2}$
	$E^{+9} + E^{+7}$	44.0 ± 0.6	$10^{21.1\pm0.3}$
E_2^{+17}	$E^{+12} + E^{+5}$	41.1 ± 2.4	$10^{20.1\pm1.3}$
	$E^{+11} + E^{+6}$	40.6 ± 1.3	$10^{19.9\pm0.7}$
	$E^{+10} + E^{+7}$	39.9 ± 0.7	$10^{19.5\pm0.4}$
	$E^{+9} + E^{+8}$	41.0 ± 1.8	$10^{20.0\pm1.0}$

[a]The Arrhenius parameters were estimated from three kinetic points spanning a 12 °C temperature range.

available and only rough estimates are included in Table 2.

From the Arrhenius plots, it is clearly seen that electrostatic effects influence the stability of the dimer ions. The kinetic stability of the dimer, while somewhat sensitive to the charge distribution, decreased with increasing charge state. The trend in kinetic stability reflects the trend in the E_a's, which decreased with increasing charge state: ~60 kcal/mol (+14), 48–50 (+15), 44–46 kcal/mol (+16) and ~41 kcal/mol (+17). A similar decrease in E_a with charge state was observed for the loss of subunit from the B_5^{n+} ions [7]. For E_2^{15+} and E_2^{16+}, the reactivity of the dimers was sensitive to the distribution of charge between the monomers, with increasing charge asymmetry leading to increased reactivity. For E_2^{15+}, the Arrhenius parameters for the dissociation of the $E^{8+}{\cdot}E^{7+}$ and $E^{9+}{\cdot}E^{6+}$ charge isomers were identical within experimental error (E_a = 50.6 ± 0.9 kcal/mol, A = $10^{24.2\pm0.4}$ s^{-1} and E_a = 50.4 ± 1.7 kcal/mol and A = $10^{24.0\pm0.8}$ s^{-1}, respectively). For the $E^{10+}{\cdot}E^{5+}$ isomer, the Arrhenius parameters were slightly smaller (E_a = 47.5 ± 1.5 kcal/mol, A = $10^{23.0\pm0.8}$ s^{-1}) but the rate constant was distinctly larger. The Arrhenius parameters were the same within the experimental error for the $E^{9+}{\cdot}E^{7+}$ and $E^{10+}{\cdot}E^{6+}$ isomers of E_2^{16+}($E_a \approx 45$ kcal/mol, A ≈ 10^{22} s^{-1}). Arrhenius parameters were not reported for the dissociation of the $E^{11+}{\cdot}E^{5+}$ isomer because of considerable scatter in the kinetic data. For E_2^{17+}, the Arrhenius parameters measured for the individual pathways were identical within experimental error ($E_a \approx 41$ kcal/mol, A ≈ 10^{20} s^{-1}).

As discussed previously, the dissociation E_a measured for noncovalent protein complexes is believed to reflect the number and strength of the noncovalent intermolecular interactions stabilizing the complex [7, 19]. Electrostatic repulsion, arising from the presence of multiple charges, will influence the stability of the dimer in two ways. First, direct repulsion between the monomers may assist in overcoming the intermolecular hydrogen bonds. Increased repulsion between the two monomers is expected to result in the cleavage of some of these noncovalent interactions and a concomitant reduction in the dissociation E_a. The magnitude of the repulsion will depend on the total number of charges, their distribution, and location on the proteins. For a homodimer such as ecotin, electrostatic repulsion between the monomers is expected to be greatest when the charge is evenly shared between the monomers, assuming that the monomers have similar conformations [4, 6]. Secondly, repulsion within each monomer can induce partial or complete unfolding of the monomers, with higher monomer charge states leading to a greater degree of unfolding. The disruption of higher order structure required for intermolecular interactions can also affect the stability of the complex. Both inter- and intra-monomer repulsion will tend to increase with increasing charge state of the dimer, resulting in a decrease in the dissociation E_a.

Within the precision of the Arrhenius parameters, the charge distribution has little or no effect on the dissociation E_a's for the charge isomers of ecotin. The only obvious effect is in the case of the E_2^{15+} isomers, where the more charge-asymmetric isomer has the smallest E_a, by ~3 kcal/mol. Douglas and coworkers have suggested that the dissociation E_a of a protein dimer will be greatest when the charge is evenly distributed between the monomers [5]. The rationale for this argument is that the symmetric charge distribution will lead to greater electrostatic repulsion between the monomers and that this greater repulsion contributes to the energy barrier to dissociation. While the trend in the E_a's measured for the E_2^{15+} isomers is in agreement with this prediction, we believe that this model is overly simplistic as it only considers the contribution of electrostatic repulsion to the energy of the transition state and not to the reactant, where it is expected to be even more significant, and ignores possible differences in the conformation of the monomers. Furthermore, it does not hold for E_2^{17+}, where there is no observable difference in the E_a's of the four isomers. We believe that differences (or similarities) in the dissociation E_a's measured for the different charge isomers reflect primarily the influence of charge distribution on the structure of the monomers and the inter-monomer interactions. For example, the lower E_a measured for the $E^{10+}{\cdot}E^{5+}$ isomer compared with $E^{9+}{\cdot}E^{6+}$ and $E^{8+}{\cdot}E^{7+}$ may reflect greater unfolding of the E^{10+} monomer, resulting in greater disruption of the inter-monomer interactions. The comparable reactivity and E_a's for the four E_2^{17+} charge isomers suggest that both monomers are significantly unfolded, due to the high overall charge state of the dimer, such that the electrostatic repulsion between the monomers is similar for all four isomers.

Conclusions

The BIRD technique has been used to investigate the thermal decomposition of the gaseous ecotin dimer ions, E_2^{n+} where n = 14–17. This is the first such study of a gaseous protein dimer. The dominant reaction for the E_2^{n+} ions at temperatures of 126 to 175 °C was dissociation into a pair of monomer ions. Dissociation of the dimer ions produced monomer ion pairs with a distribution of charge states, ranging from symmetric (or nearly symmetric in the case of the odd charge state dimers) to highly asymmetric with one of the monomers retaining as much as 71% of the total charge. For E_2^{14+}, E_2^{15+} and E_2^{16+}, the relative abundance of the monomer ions measured at ~100% reaction was independent of temperature. Based on this result, it was concluded that little or no proton transfer takes place between the monomers during dissociation and that the distribution of monomer charge states arises from the presence of charge isomers of the dimer, which differ in the number of charges associated with each monomer. It was further concluded that the charge isomers originated in the nanoES ion source, likely as a consequence of the nanoES/desolvation process. For the E_2^{17+} ion,

there was evidence of thermally-assisted proton transfer between monomers, with higher reaction temperatures favoring a more symmetric distribution of charge. Although additional dissociation studies of homo- and heterodimers are necessary, the present results suggest that the nanoES process may result in gaseous protein dimers with a distribution of monomer charge states. Consequently, the general observation of highly asymmetric monomer charge states in the CID spectra of protein dimers [4, 5] may result, in part, from the dissociation of asymmetric charge isomers produced by the ES (nanoES) process. It is likewise possible that gaseous multimeric protein complexes produced by ES also consist of multiple charge isomers.

In addition to the dissociation of the dimer ions into monomers, two other reaction pathways were observed. The dimer ions were found to undergo loss of one or more neutral molecule(s), believed to be H_2O or NH_3. The dimer ions were also susceptible to proton transfer to residual neutrals in the vacuum chamber, resulting in the appearance of $E_2^{(n-1)+}$ ions in the BIRD spectra.

The kinetic stability of the dimer ions was clearly influenced by electrostatic effects. Reactivity was governed primarily by the charge state of the dimer, with higher charge states promoting dissociation; the partitioning of charge between monomers had a small or no effect on reactivity. For the charge isomers of E_2^{15+} and E_2^{16+}, the dissociation rate constants increased with the degree of charge asymmetry, a result that was attributed to increased unfolding of the high charge state monomer and disruption of some of the inter-monomer interactions. In contrast, identical rate constants were measured for the charge isomers of E_2^{17+} ions, suggesting that at the +17 charge state, both monomers were significantly unfolded, such that differences in electrostatic effects for the different charge isomers were negligible. The rate constants for the dissociation of E_2^{n+} charge isomers ions into monomers were determined from the time-resolved BIRD spectra. Extracting rate constants from the kinetic data was complicated by the parallel charge and neutral loss reactions, as well as coincidental *m/z* values for some of the ions, and several simplifying assumptions were necessary. Estimates of the Arrhenius parameters for the dissociation of the dimer ions were obtained from the temperature dependence of the rate constants. For the charge isomers of E_2^{15+}, the E_a, and A-factors are slightly sensitive to the charge distribution, decreasing with increasing charge asymmetry, while for the charge isomers of E_2^{17+}, the Arrhenius parameters were identical.

Future studies will examine the dissociation behavior of other homo- and heterodimers to establish whether the results obtained for ecotin are general and whether a higher order protein structure influences the distribution of the charge and the dissociation pathways, kinetics, and energetics.

Acknowledgments

The authors are grateful for financial support provided by the Natural Sciences and Engineering Research Council of Canada (NSERC). They thank A. Blades for helpful discussions during the preparation of this manuscript.

References

1. Goodsell, D. S.; Olson, A. J. *Annu. Rev. Biophys. Struct.* **2000,** *29,* 105–153.
2. Jones, S.; Thornton, J. M. *Proc. Natl. Acad. Sci. U.S.A.* **1996,** *93,* 13–20.
3. Loo, J. A. *Int. J. Mass Spectrom.* **2000,** *200,* 175–186.
4. Versluis, C.; van der Staaij, A.; Stokvis, E.; Heck, A. J. R. *J. Am. Soc. Mass. Spectrom.* **2001,** *12,* 329–336.
5. Mauk, M. R.; Mauk, A. G.; Chen, Y.-L.; Douglas, D. J. *J. Am. Soc. Mass. Spectrom.* **2002,** *13,* 59–71.
6. Light-Wahl, K. J; Schwartz B. L.; Smith R. D. *J. Am. Chem. Soc.* **1994,** *116,* 5271–527.
7. Felitsyn, N.; Kitova, E. N.; Klassen, J. S. *Anal. Chem.* **2001,** *73,* 4647–4661.
8. Zhang, Z.; Krutchinsky, A.; Endicott, S.; Realini, C.; Rechsteiner, M.; Standing, K. G. *Biochemistry* **1999,** *38,* 5651–5658.
9. (a) Dunbar, R. C.; McMahon, T. B. *Science* **1998,** *279,* 194–197. (b) Price, W. D.; Williams, E. R. *J. Phys. Chem.* **1997,** *101,* 8844–8852.
10. Chung, C. H.; Ives, H. E.; Almeda, S.; Goldberg, A. L. *J. Biol. Chem.* **1983,** *258,* 11032–11038.
11. Shin, D. H.; Song, H. K.; Seong, I. S.; Lee, C. S.; Chung, C. H.; Suh, S. W. *Protein Sci.* **1996,** *5,* 2236–2247.
12. Seymour, J. L.; Linquist, R. N.; Dennis, M. S.; Moffat, B.; Yansura, D.; Reilly, D.; Wessinger, M. E.; Lazarus, R. A. *Biochemistry* **1994,** *33,* 3949–3958.
13. (a) McGrath, M. E.; Erpel, T.; Bystroff, C.; Fletterick, R. J. *EMBO J* **1994,** *13,* 1502–1507. (b) Pal, G.; Szilágyi, L.; Gráf, L. *FEBS Lett* **1996,** *385,* 165–170.
14. Jarrold, M. F. *Annu. Rev. Phys. Chem.* **2000,** *51,* 179–207.
15. (a) Jockusch, R. A.; Schnier, P. D.; Price, W. D.; Strittmatter, E. F.; Demirev, P. A.; Williams, E. R. *Anal. Chem.* **1997,** *69,* 1119–1126. (b) Huang, Y. L.; Pasatolic, L.; Guan, S. H.; Marshall, A. G. *Anal. Chem.* **1994,** *66,* 4385–4389.
16. Dole, M.; Mack, L. L.; Hines, R. L.; Mobley, R. C.; Ferguson, L. D.; Alice, M. B. *J. Chem. Phys.* **1968,** *49,* 2240.
17. de la Mora, J. F. *Anal. Chim. Acta* **2000,** *406,* 93–104.
18. Nagradova, N. K. *FEBS Lett.* **2001,** *487,* 327–332.
19. Kitova, E. N.; Bundle, D. R.; Klassen, J. S. *J. Am. Chem. Soc.* **2002,** *124,* 5902–5913.